

Research Paper

SENP1 Interacts with HIF1 α to Regulate Glycolysis of Prostatic Carcinoma Cells

Chunyang Wang¹✉, Weiyang Tao², Shaobin Ni¹, Qiyin Chen¹

1. Department of Urology, the First Affiliated Hospital of Harbin Medical University, Harbin, China
2. Department of Breast Surgery, the Third Affiliated Hospital of Harbin Medical University, Harbin, China

✉ Corresponding author: Chunyang Wang, Address: Department of Urology, The First Affiliated Hospital of Harbin Medical University, 23 Youzheng Street, Harbin 150001, China. Tel/Fax: +86 451 8555 5086; Fax: +86 451 8555 5086; E-mail: WangChunYang2018@yeah.net

© Ivyspring International Publisher. This is an open access article distributed under the terms of the Creative Commons Attribution (CC BY-NC) license (<https://creativecommons.org/licenses/by-nc/4.0/>). See <http://ivyspring.com/terms> for full terms and conditions.

Received: 2018.05.14; Accepted: 2018.12.03; Published: 2019.01.01

Abstract

Background: Hypoxic microenvironment inside the tumor forces tumor cells to up-regulate the glycolytic pathway to maintain a sufficient energy supply for tumor growth. Activation of HIF1 α under hypoxia condition is able to regulate the expression of glycolysis-related genes, and results in the proliferation and metastasis of cancer cells. However, the mechanism underlying HIF1 α activation and glycolysis induction by hypoxia remains unclear. The present study is aimed to test if SENP1 regulates the glycolysis of prostate cancer cells (CaP) by improving stability of HIF1 α protein.

Methods: We employed qPCR and western blotting assay to analyze expression of HIF1 α and SENP1. Glucose uptake assay, lactate production assay, LDH release assay and ATP production assay were utilized to evaluate cell glycolysis. The interaction between SENP1 and HIF1 α was verified by co-immunoprecipitation assay.

Results: We found that hypoxia condition improves glucose uptake and lactate production to sustain sufficient ATP for cellular activity in prostatic carcinoma cells. The expression of SENP1 mRNA was significantly increased in human prostatic carcinoma cell lines after exposure to hypoxia, accompanied by the up-regulation of HIF1 α . Furthermore, forced expression of SENP1 was shown to regulate the glycolysis in prostatic carcinoma cells by stabilizing HIF1 α . The up-regulation of SENP1 promotes tumor cell proliferation and tumorigenesis by interacting with HIF1 α which was deSUMOylated and sequentially leading to a "Warburg effect".

Conclusion: SENP1 interacts with HIF1 α to regulate glycolysis and proliferation of prostatic carcinoma cells under hypoxia condition, which provides new insights into prostatic carcinoma therapy.

Key words: SENP1, HIF1 α , glycolysis, prostatic carcinoma, tumorigenesis.

Introduction

Cancer cell metabolism is usually different from normal cells, which is characterized by the enhanced conversion of glucose to lactate. Cancer cells largely depend on the glycolytic pathway to maintain the energy production even in the presence of an adequate oxygen supply. This typical metabolic feature on multiple cancer cells is later termed as the Warburg effect (aerobic glycolysis) [1-3]. Now, Warburg effect has been widely recognized as a hallmark of cancer cell metabolism which can

facilitate tumor growth with enhanced glucose uptake and lactate production [4]. Warburg effect makes tumor cells survive and proliferate in a unique microenvironment, thereby promoting apoptosis tolerance, increasing the formation of biosynthetic precursor molecules and enhancing the invasiveness of the biosynthetic precursors, and making the tumor cells progressed and metastases. Therefore, the understanding of this process is crucial to identify new potential targets for prostatic carcinoma therapy.

A large body of evidence uncovers that hypoxia stimulates lactate production in tumors by activating hypoxia-inducible transcription factor 1 α (HIF1 α)-dependent expression of genes including glucose transporter 1 (GLUT1), pyruvate dehydrogenase kinase 1 (PDK1), and lactate dehydrogenase A (LDHA) and so on. These genes are involved in glycolysis, lactic acid generation, aerobic respiration, mitochondrial autophagy and a variety of cellular functions [5-8]. It has been showed that the expression of HIF1 α was increased significantly in prostatic carcinoma cells, which is closely associated with the proliferation and metastasis of prostatic carcinoma [9-11]. But the molecular mechanism of HIF1 α up-regulation in prostatic carcinoma has not been elucidated yet.

HIF1 α has an extremely short half-life under normoxia condition due to the ubiquitylation and degradation by the proteasome [12]. SUMOylation modulates DNA replication/repair, cell cycle progression, signal transduction, and the hypoxic response. SUMO (small ubiquitin-like modifier)-specific proteases regulate SUMOylation. In addition, deSUMOylation has also been shown to play a critical role in tumorigenesis via HIF1 α -dependent angiogenesis and cell proliferation [11]. Mechanistic studies in a mouse model indicate that androgen-driven expression of SUMO1/sentrin specific peptidase 1 (SEN1) leads to HIF1 α stabilization, enhanced production of vascular endothelial growth factor, and angiogenesis [11]. Some studies showed that up-regulation of SEN1 at the mRNA and protein level might contribute to the malignant progression of CaP cells [13]. However, the role of SEN1 in the up-regulation of HIF1 α in prostatic carcinoma has not been clarified clearly.

In the current study, we found that prostatic carcinoma display a greater sensitivity to glucose deprivation-induced cytotoxicity than normal cells. The up-regulation of SEN1 in prostatic carcinoma cells induced cellular proliferation by promoting HIF1 α . It indicates that the inhibitors of glucose cellular uptake (facilitative glucose transporter 1 inhibitors) and oxidative metabolism (glycolysis inhibitors) are potential therapeutic targets for prostatic carcinoma treatment.

Materials and Methods

Cell culture and reagents

Du145, LNCap, PC3, 22RV1, C4-2 prostatic carcinoma cell lines and normal prostatic epithelial cell line-RWPE-1 cells were bought from the Guangzhou Landsales Biological Science and Technology Co.,Ltd, which were purchased from the

American Type Culture Collection (ATCC) (Manassas, VA, USA). Cells were cultured in RPMI-1640 (#SH30809.01B, Hyclone) supplemented with 10% fetal calf serum (Hyclone, USA) and 1% penicillin/streptomycin (Hyclone, USA). All cells were maintained at 37°C in a humidified 5% CO₂ incubator. All cells were cultured in normoxic (O₂ 20%), hypoxic conditions (O₂ 1%), anoxic (O₂ 0.1%), low pH (pH 3-4) and glucose deprivation (glucose-free medium) for 24h in a 37°C CO₂ incubator to perform experiments.

PC3 cells were transfected with indicated plasmids or SEN1 siRNAs, which purchased from Sangon Biotech, China. PC3 cells at approximately 50% confluence were transfected using Lipofectamine 2000 (Invitrogen, USA) according to manufacturer's guidelines. Si-SEN1, si-NC and mock1 group PC3 cells were transfected with 50 nM si-SEN1, 50 nM negative controls or the empty vector. SEN1 and mock2 group PC3 cells were transfected with 50 nM SEN1 or its empty vector, respectively. Cells were maintained in high glucose Dulbecco's modified Eagle's medium (DMEM; Gibco, USA) supplemented with 10% FBS and 1% penicillin-streptomycin, which were maintained in an incubator with 5% CO₂ in humidified atmosphere at 37°C. The transfected efficiency of these plasmids or siRNAs was further validated by qRT-PCR assay and western blot assay.

qRT-PCR analysis

Total RNA of all cells were extracted by Trizol (Invitrogen, USA), followed by reverse transcription with a reverse transcription PCR Kit (Applied Biosystems, USA). The real-time polymerase chain reaction (RT-PCR) was performed using real-time PCR Master Mix (Toyobo, Japan) according to the manufacturer's instruction on an ABI PRISM 7500 Sequence Detection System (Applied Biosystems, USA). The PCR amplification program was 95°C 5 min, (95°C 15 sec, 65°C 30 sec, 72°C 30 sec, 40 cycles) and followed by dissociation curve protocol (95°C 15 sec, 60°C 1 min, 95°C 15 sec, and 60°C 15 sec). 18S rRNA was used as the internal control. We determined the appropriate cycle threshold (Ct) using the automatic baseline determination feature. The relative quantification of gene expression level was analyzed by the comparative Ct method ($2^{-\Delta\Delta Ct}$). All primer pairs used in this study are listed in table-1.

Western blot analysis

Cells were harvested from different groups. Total proteins were extracted using RIPA lysis buffer and Protease Inhibitor Cocktail. Lysates (80 μ g) were separated by 10% sodium dodecyl sulfate-polyacrylamide (SDS-PAGE) gels for electrophoresis

with procedure of 80V, 50 min, then 120V to the end at room temperature and transferred to nitrocellulose membrane (0.22 μm , Millipore, USA) by wet blotting procedure (100V, 120 min, 4°C). Membranes were incubated with specific primary antibodies of SENP1 (Proteintech Group, Inc. 25349-1-AP, Rosemont, IL, USA) (1:1000) and HIF1 α (Abcam, ab1, Cambridge, MA, USA) (1:1500) overnight at 4°C. GAPDH (KangChen Bio-tech. KC-5G5, Shanghai, China) (1:10000) was used as an internal control. Proteins were visualized by enhanced chemiluminescence reagents (Beyotime, China) and photographed by GelDoc⁺ XR instrument (BioRad, USA).

Table 1. The sequences of primer pairs for qRT-PCR

	Primer	Primer Sequence (5'-3')
SENP1	Forward	CAGCAGATGAATGGAAGTGA
	Reverse	CCGGAAGTATGGCATGTGT
HIF1 α	Forward	GTGGATTACCACAGCTGA
	Reverse	GCTCAGTTAACTTGATCCA
18S	Forward	CCTGGATACCCGAGCTAGGA
	Reverse	GCGGCGCAATACGAATGCCCC

Co-immunoprecipitation (Co-IP) assay

A Co-IP assay was performed to determine the relationship between SENP1/HIF1 α , HIF1 α /SUMO1 and HIF1 α /MCT4. The Co-IP kit was used according to the manufacturer's protocol. Briefly, cells seeded in 10-mm dishes were lysed in 1 ml cell lysis buffer. 500 μg proteins were incubated with 2 μg of the indicated antibodies overnight at 4°C under gently rotation, and then they were incubated with 30 μl Protein G-Sepharose beads (Abcam, USA) at 4°C for 2h under rotation. The beads were washed three times with the lysis buffer and resuspended in SDS sample buffer, boiled for 10 min, and then analyzed by immunoblotting procedures described above.

Glucose uptake, lactate, ATP and lactate dehydrogenase (LDH) release assays

Glucose uptake assay kit (Shanghai Rong Sheng Biological Pharmaceutical Co., Ltd., China), lactate assay kit (Nanjing JianCheng Bioengineering Institute, China) and ATP assay kit (Beyotime, China) were made use of evaluating glucose uptake, lactate production and ATP generation respectively, according to the manufacturer's instructions. The evaluation of LDH release was performed with a LDH Cytotoxicity Assay Kit (Beyotime, China) according to the manufacturer's manuals. For lactate assay, the harvested cells were directly used to examine the lactate levels with the lactate assay kit. The chemiluminescence was measured to determined ATP levels of each group cells, which based on the luciferin-luciferase reaction.

Tumor xenograft model

This experiment was approved by the Ethic Committee for Animal Experimentation of the First Affiliated Hospital of Harbin Medical University. Male athymic BALB/c nude mice (4 weeks old, 15-20 g weight) were purchased from Shanghai SLAC Laboratory Animal Ltd.Co. (Shanghai, China). Mice were housed in barrier facilities on a 12h light/dark cycle and maintained under super-specific pathogen-free conditions. A total of 5×10^6 tumor cells suspended in 200 μL PBS were inoculated subcutaneously in four-week-old male BALB/c athymic nude mice. Within 3 weeks, xenograft tumors were established, and the sizes of tumors were measured by a digital caliper every 3 days. The mice were then randomly assigned into groups as mentioned in the text. Tumor volumes (mm^3) were calculated using the following standard formula: Tumor volumes (mm^3) = (the longest diameter) \times (the shortest diameter)² \times 0.5.

H&E staining

Mice were sacrificed by CO₂ inhalation at 22 days post-injection and tumors were excised. The dissected tumors were immediately fixed in 4% paraformaldehyde, processed for paraffin embedding, and cut into the 4 μm sections. The paraffin sections were deparaffined and then they were dyed using hematoxylin-erosin (H&E) for pathological analysis. An OLYMPUS inverted microscope was used to capture the staining results. Quantitative morphometric assessments of tumor cells were performed using Image-Pro Plus 6.0 (Media Cybernetics, Bethesda, MA, USA). The tumor cells densities were calculated as tumor cells area per total tissue area in each field.

Statistical analysis

Each experiment was performed at least three independent batches and data are shown as the mean \pm standard deviation (S.D.). Statistical analyses were performed by SPSS software version 13.0 (SPSS Inc., Chicago, USA). Differences were estimated with one-way analysis of variance (ANOVA). All of the figures were plotted using GraphPad Prism (GraphPad Software Inc., San Diego, USA). Differences with $P < 0.05$ were considered to be statistically significant.

Results

Induction of aerobic glycolysis in prostatic carcinoma cells

Warburg effect (aerobic glycolysis) is characterized by elevated glucose uptake and

consumption with high-lactate production even in the presence of oxygen [14]. To confirm the correlation between aerobic glycolysis and cell microenvironment, we exposed human prostatic carcinoma cell lines Du145, LNCaP, PC3, 22RV1, C4-2 cells and human prostatic epithelial cell line RWPE-1 cells to four kinds of cell microenvironments including hypoxia, anoxia, low pH and nutritional deficiency. Firstly, we investigated the morphological changes of these cells after exposed to different pathological conditions. As shown in Figure 1A, the cellular morphology was not altered in hypoxia, anoxia, low pH and nutritional deficiency treatment in RWPE-1 cells, but significantly altered in human prostatic carcinoma cell lines in different degrees. The result indicated that there were remarkably differences between normal cells and tumor cells in response to different treated conditions. Then we investigated the difference of glucose uptake, lactate and ATP production, and lactate dehydrogenase (LDH) release between cancer cells and normal cells. As shown in Figure 1B-C, compared with RWPE-1 cells, glucose uptake and lactate production were significantly increased in human prostatic carcinoma cell lines after treatment with hypoxia. Additionally, LDH release was significantly higher in human

prostatic carcinoma cell lines than RWPE-1 cells (Figure 1D) and the ATP production was significantly increased in 22RV1 and C4-2 human prostatic carcinoma cell lines with the above treatments, whereas there was no significant difference of ATP production was found in DU145, LNCaP and PC3 human prostatic carcinoma cell lines after treatment with all the above conditions (Figure 1E). These data indicates that prostatic carcinoma cells have the increased glucose uptake and lactate production to sustain sufficient ATP for cellular activity under hypoxic, anoxic, low pH and nutritional deficiency conditions.

Up-regulation of HIF1 α and SENP1 expression in human prostatic carcinoma cells

HIF1 is an important transcription factor for tumor energy metabolism [15], and SENP1 is highly expressed in human prostate cancer specimens and correlates with HIF1 α expression [11]. Hence, we further investigated the expression of HIF1 α and SENP1 in human prostatic carcinoma cell lines with different pathological stimuli. As expected, the expression level of HIF1 α mRNA in 22RV1, Du145, LNCaP and PC3 cells was obviously higher than that in RWPE-1 cells after hypoxic and anoxic treatment

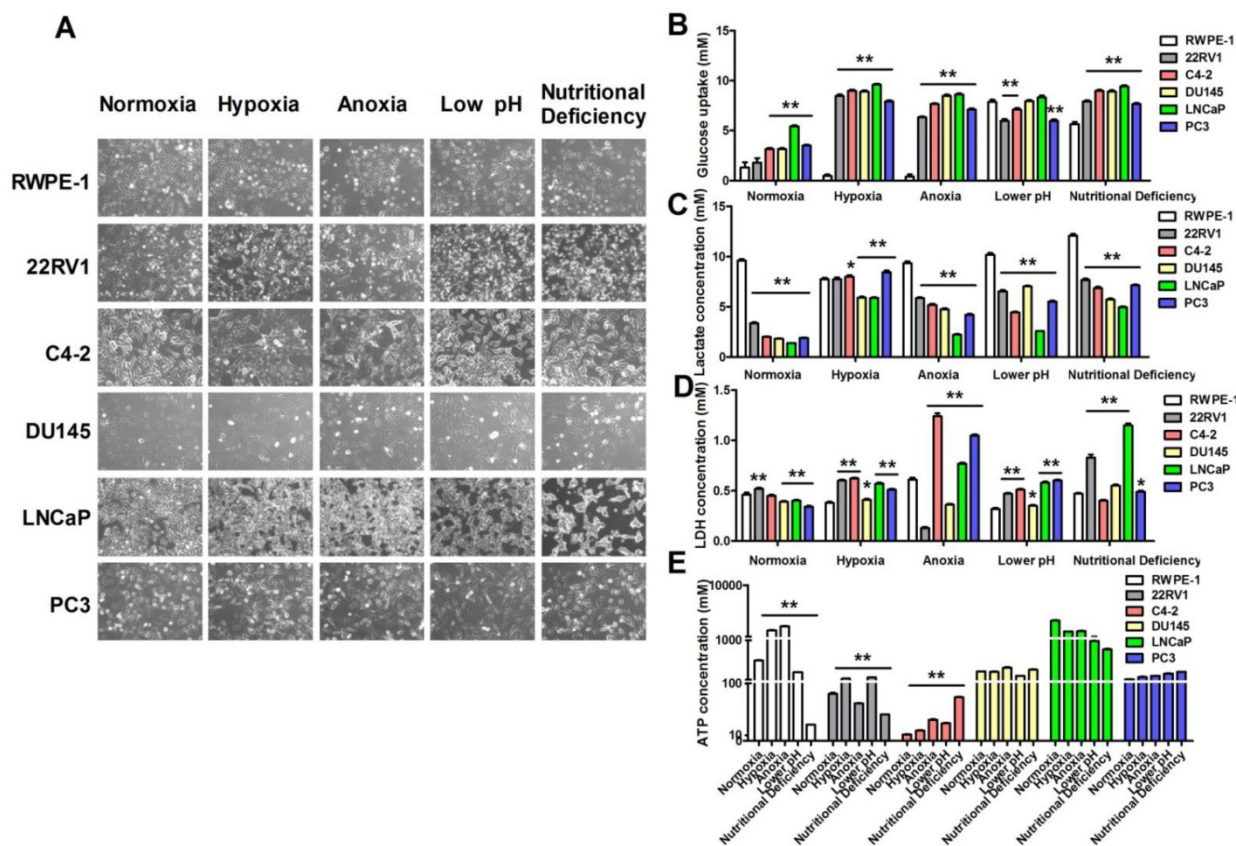


Figure 1. Hypoxia conditions promote prostatic carcinoma cell glycolysis. (A) Morphology changes of human prostatic epithelial cell and prostatic carcinoma cell lines subjected to the treatments of different conditions. (B-E) Extreme conditions can improve glucose uptake (B), lactate production (C), LDH release (D) and ATP production (E) of prostatic carcinoma cells. * $P < 0.05$ vs. RWPE-1 cells, ** $P < 0.01$ vs. RWPE-1 cells or normoxia group cells.

but not low pH and nutritional deficiency treatment (Figure 2A). Meanwhile, the mRNA expression of SENP1 was also significantly increased by hypoxia and anoxia but not low pH and nutritional deficiency in 22RV1, DU145, LNCaP and PC3 cells (Figure 2B). Then we further detected the abundance of HIF1 α and SENP1 protein in 22RV1, C4-2, DU145, LNCaP and PC3 human prostatic carcinoma cell lines and RWPE-1 human prostatic epithelial cell line (Figure 2C). The result showed that both HIF1 α and SENP1 proteins were more abundant in five human prostatic carcinoma cell lines, especially the higher in PC3 cells than other cells. Hence, HIF1 α and SENP1 are expressed most abundantly in PC3 cells. Consistently, PC3 cells are more sensitive to extracellular microenvironments of hypoxia and anoxia than other cells (Figure 1A-C). Thus, we chose PC3 cells as experiment cells for the following studies.

SENP1 regulates cell glycolysis through stabilizing HIF1 α

Previous studies demonstrated that the expression of SENP1 was positively associated with glycolysis levels in clear cell renal cell carcinoma [16], so we studied whether SENP1 might regulate glycolysis of PC3 cells through HIF1 α . In order to confirm the hypothesis, we performed SENP1

knockdown and overexpression experiments in PC3 cells. Firstly, we constructed stable PC3 cell lines, including SENP1 PC3 cells (SENP1), NC PC3 cells (NC), mock1 PC3 cells (mock1), mock2 PC3 cells (mock2), si-NC PC3 cells (si-NC) and si-SENP1 PC3 cells (si-SENP1), and the SENP1 and HIF1 α expressions in mRNA and protein levels were identified by qRT-PCR assay and western blot assay (Figure 3A-3C) to verify whether these stable cell lines were successfully established. It was found that the mRNA and protein expression levels of SENP1 were decreased in si-SENP1 PC3 cells, and the mRNA and protein expression levels of HIF1 α were correspondingly decreased, which implied that there was a potential regulatory relationship between SENP1 and HIF1 α . Subsequently, to demonstrate the interaction of SENP1 and HIF1 α , Co-IP assay was performed. The result uncovered that SENP1 directly interact with HIF1 α (Figure 3D). Previous studies have suggested that SENP1 may regulate the expression of its target proteins by deSUMOylation [17]. Thus, it indicates that SENP1 enhanced the stability of HIF1 α probably by deSUMOylation pathway to regulate glycolysis in human prostatic carcinoma cell lines.

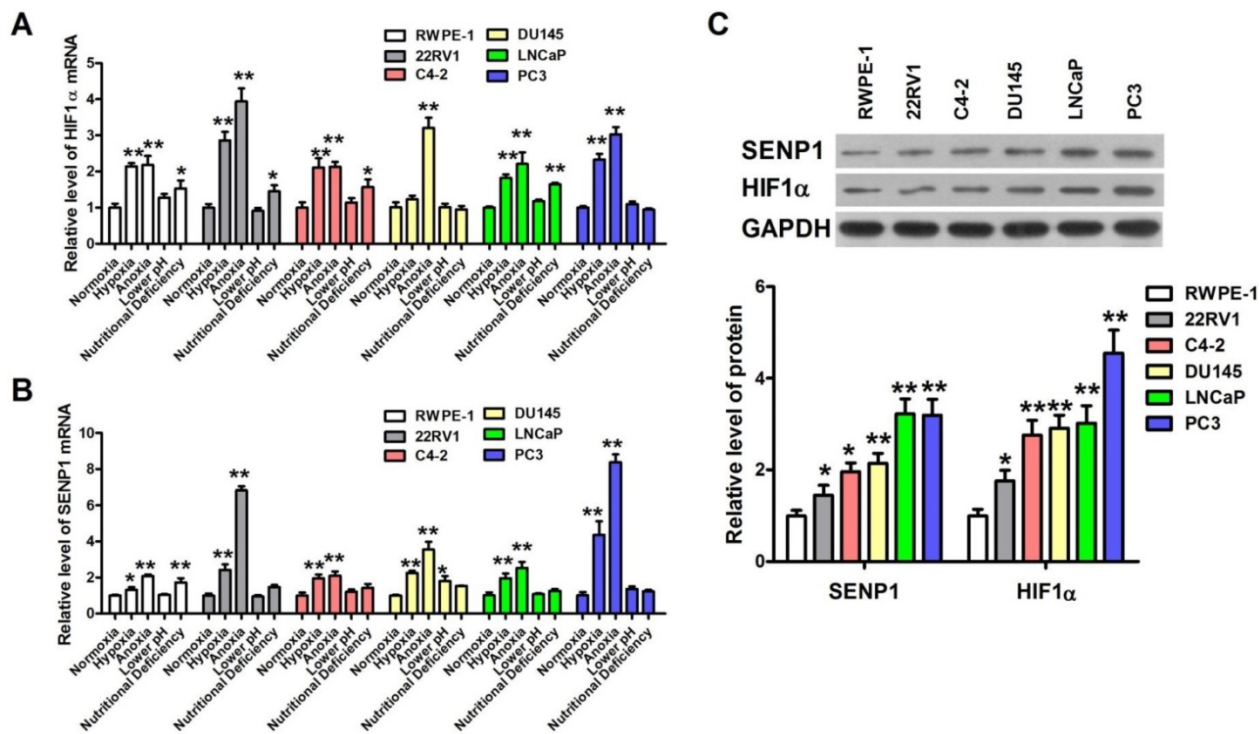


Figure 2. Hypoxia induces up-regulation of HIF1 α and SENP1 in human prostatic carcinoma. (A) HIF1 α mRNA expression was increased in human prostatic carcinoma cells lines after treatment with hypoxia, anoxia and nutritional deficiency conditions. Especially, after treatment with hypoxia and anoxia, the expression of HIF1 α mRNA was increased significantly in all the human prostatic carcinoma cells lines. (B) SENP1 mRNA expression was elevated in all the four extreme conditions of human prostatic carcinoma cells lines. Exposure to hypoxia and anoxia significantly increased the expression of SENP1 mRNA in all the human prostatic carcinoma cells lines. (C) The protein abundance of HIF1 α and SENP1 in human prostatic carcinoma cells lines and human prostatic epithelial cell line RWPE-1 cells. * $P < 0.05$ vs. normoxia group cells or RWPE-1 cells, ** $P < 0.01$ vs. normoxia group cells or RWPE-1 cells.

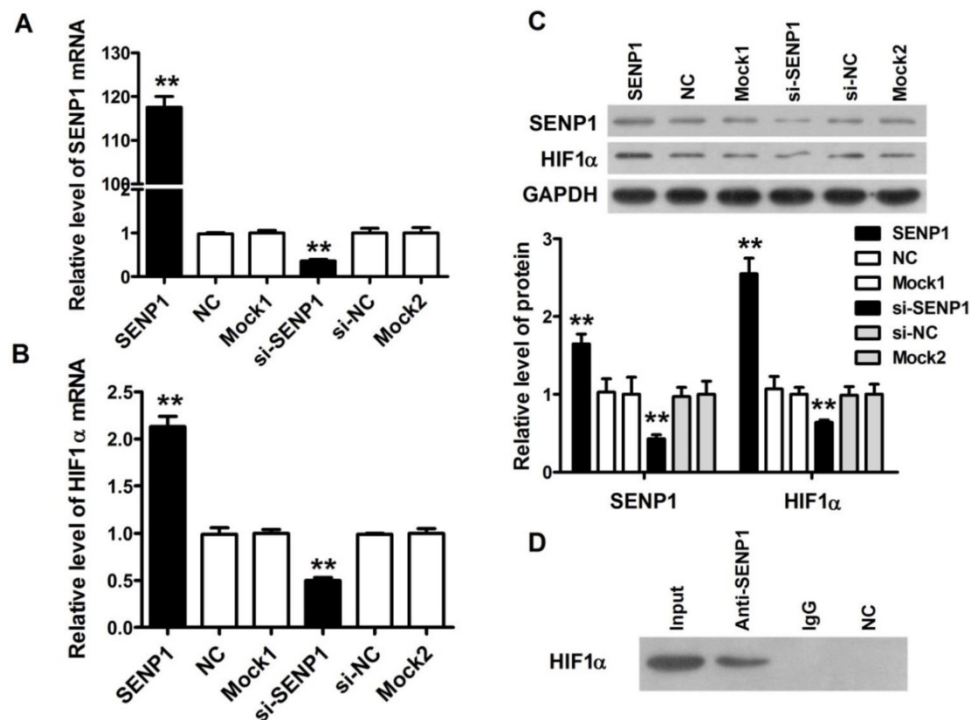


Figure 3. SENP1 regulates cell glycolysis through stabilizing HIF1α. The SENP1 and HIF1α expression at mRNA (A, B) and protein (C) levels were measured by qRT-PCR and Western Blot assay in PC3 cells transfected with SENP1, NC, mock1, si-SENP1, si-NC and mock2 plasmids. (D) The interactions between SENP1 and HIF1α were analyzed by Co-IP. ** $P < 0.01$ vs. NC PC3 cells, # $P < 0.01$ vs. si-NC PC3 cells.

Up-regulation of SENP1 promotes tumorigenesis *in vivo*

To further determine the role of SENP1 in the progression of tumor, tumor xenograft models were established with PC3 cells of wild type PC3 cells (NC), si-SENP1, mock1, si-NC, SENP1 and mock2 PC3 cells injection. The results demonstrated that the tumors were formed in all groups from the fourth day after tumor cells inoculation. During a three-week follow-up period, it was observed that the tumor volumes were gradually increased with time prolonged (Figure 4A). On day 22, the sizes of tumors were larger in SENP1 overexpression group than those in no transfection group (NC), while the tumors were smaller in si-SENP1 group than those in si-NC group PC3 cells (Figure 4B). Furthermore, H&E staining showed that more cells presented in SENP1 overexpression group, but fewer cells appeared in si-SENP1 group than those in other control groups (Figure 4C). The results indicate that up-regulation of SENP1 might accelerate tumor cell growth, whereas down-regulation of SENP1 decelerates tumor cell growth.

SENP1 deSUMOylates HIF1α and promotes Warburg effect

The correlations of SENP1 and hypoxia-induced tumor progression prompted us to investigate how SENP1 regulates HIF1α stability and transcriptional activity. It was previously reported that SENP1 was

able to deSUMOylate HIF1α and increased its stability in hypoxia. Thus, we further explore the effects of SENP1 on HIF1α SUMO modification, stability and transcriptional activity in PC3 cells. As shown in Figure 5A, SENP1 protein expression was significantly increased in PC3 cells after treatment with hypoxia and it was effectively reduced by co-transfection of si-SENP1. Consistent with the changes of SENP1, the protein level of HIF1α was increased in PC3 cells with hypoxic treatment and significantly decreased in PC3 cells with hypoxic+si-SENP1 treatment. However, the protein level of SUMO1 was opposite with the protein level of SENP1 and HIF1α (Figure 5A). Next, Co-IP assay showed that increased amounts of SUMO1-conjugated HIF1α were obviously accumulated in PC3 cells with hypoxia+si-SENP1 treatment as compared to the hypoxia group (Figure 5B). To further investigate the regulatory role of SENP1 in glycolysis process, glycolysis-related proteins were examined by western blot assay. As illustrated in Figure 5C, compared to control group, PDK1, GLUT1, MCT4, HIF1α, HKII, BNIP3 and LDHA expressions were remarkably up-regulated under hypoxic condition. Furthermore, overexpression of SENP1 could markedly promote these protein expressions. Additionally, under hypoxia+SENP1 condition, the expression levels of these proteins were further apparently elevated. Consistent with previous results, SUMO1 protein expression decreased in both hypoxia

and SENP1 overexpression group cells, and further declined significantly in hypoxia+SENP1 group. Co-IP assay revealed that MCT4 protein directly interact with HIF1 α in hypoxia condition (Figure 5D). It suggests that under normoxic condition, HIF1 α could be SUMOylated, whereas under hypoxic

condition, HIF1 α was combined with SENP1, followed by deSUMOylating, and sequentially interacted with MCT4, which eventually led to a "Warburg effect". This process was considered as an essential energy metabolism pathway which promoted cancer cells proliferation.

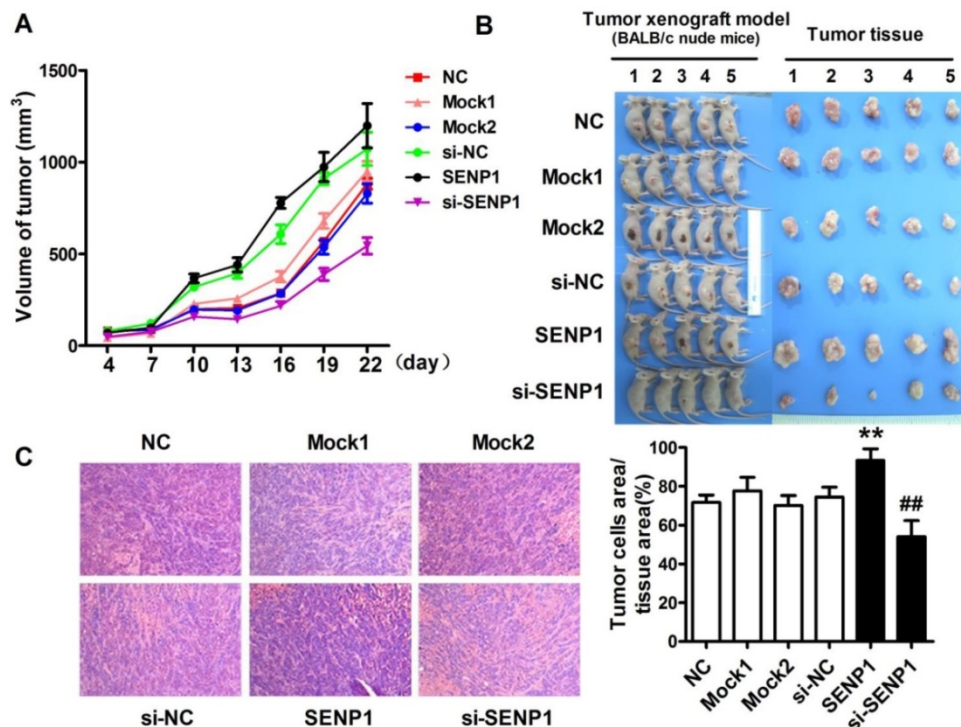


Figure 4. SENP1 promotes prostatic carcinoma growth in vivo. (A) Tumor growth curve was measured from day 4 to day 22. (B) The pictures of tumor tissues of each group xenograft model mice were taken out at day 22. (C) Hematoxylin and eosin (H&E) staining of histological sections of tumor tissues in each group (magnification 100 \times). ** $P < 0.01$ vs. NC, ## $P < 0.01$ vs. si-NC.

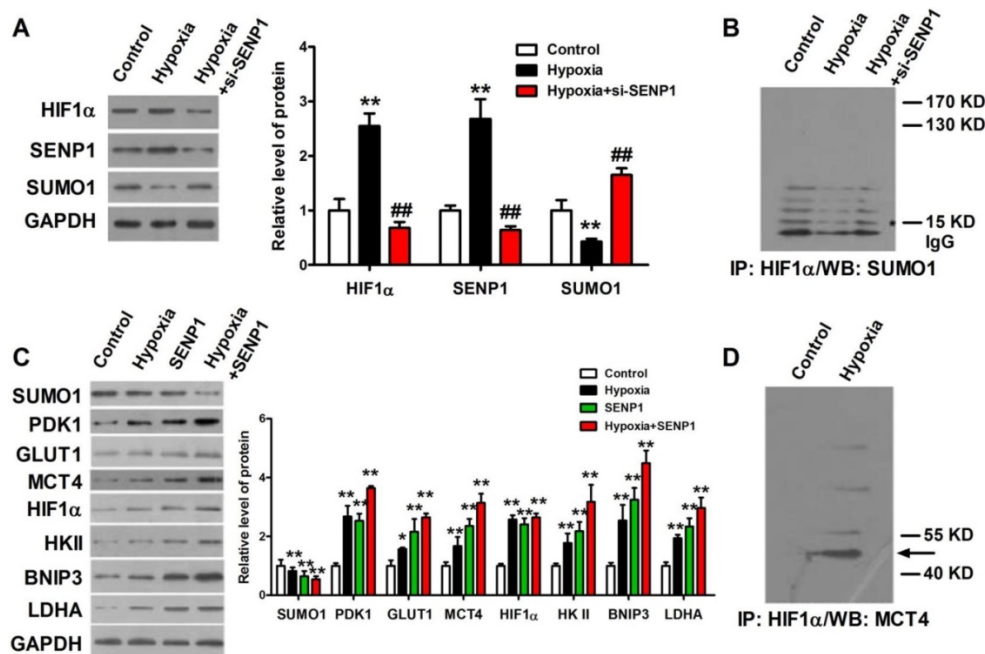


Figure 5. SENP1 deSUMOylates HIF1 α to regulate Warburg effect. HIF1 α protein was deSUMOylated by SENP1 and subsequently combined with MCT4, which finally promotes a "Warburg effect". (A) HIF1 α , SENP1 and SUMO1 proteins expressions were determined by Western Blot technique in PC3 cells treated with hypoxia or hypoxia+si-SENP1. (B) The interaction between HIF1 α protein and SUMO1 protein was examined by Co-IP assay in PC3 cells after treatment with hypoxia or hypoxia+si-SENP1. (C) SENP1 activated HIF1 α signaling pathway by regulating HIF1 α in PC3 cells after treatment with hypoxia, SENP1, and hypoxia+SENP1 respectively. (D) The interaction between HIF1 α protein and MCT4 protein was detected by Co-IP assay in PC3 cells after treatment with hypoxia. ** $P < 0.01$ vs. Control, ## $P < 0.01$ vs. Hypoxia.

Discussion

Prostate cancer presently has surpassed lung cancer as the most common malignant tumor in men in the USA [18]. But the pathogenesis of prostate cancer has not clarified clearly yet. Hypoxia commonly occurs in cancer cells, including prostate cancer cells, which is a negative prognostic factor due to its association with an aggressive tumor phenotype and therapeutic resistance [19]. Thus, hypoxia has been one of the distinguishing and near-universal hallmarks of cancer growth. It has been reported that hypoxia promotes tumor cells to develop an inefficient pathway to generate ATP which was necessary to maintain tumor rapid growth, which was termed the Warburg effect [20-21]. The Warburg effect has been recognized as a representative phenomenon in various malignant cancer cells [22]. Cell morphological examination is an intuitive observation method, which represents the most initial survival state of cells and directly display the overall performance of tumor cells at different metabolic levels, including changes in cell populations, cell morphology and cell size. Therefore, in this study, we firstly investigated human prostatic carcinoma cells morphological changes after exposed to different pathological conditions. The results showed different phenotypes between normal cells and human prostatic carcinoma cells in response to each of cell microenvironments, which suggested that the metabolic mechanism and metabolites of human prostatic carcinoma cells were significantly different from that of normal cells. Because of the basic ATP production is different between each cell line, we preformed different statistical graph of Figure 1E from Figure 1B-C to clearly display the ATP production of each cell line after expose to hypoxia, anoxia, lower pH and nutritional deficiency. Furthermore, there are some differences of cell cycle and physiological characteristics among cancer cells or between cancer cells and normal cells, the basic metabolites produced by each group of cells are different, even under normoxic cell culture condition. Therefore, as show in Figure 1B-1E, under normal oxygen conditions, the glucose uptake, LDH concentration, lactate and ATP production of each group cells were different between each other. Although several possible mechanisms have been proposed to explain this metabolic difference of tumor cells, the exact mechanisms are still not elucidated.

Hypoxic microenvironment in cancer is capable of activating HIF1 α , which is continuously synthesized and degraded under non-hypoxic conditions due to rapid hydroxylation with prolyl

hydroxylase domain (PHD) via ubiquitaytion [23], thereby the level of HIF1 α is normally low under normoxic condition. Recent studies showed that SENP1 expression was elevated in multiple carcinomas [24-25]. Consistently, our study showed that the expression levels of HIF1 α and SENP1 were remarkably increased in prostate carcinoma cell lines after cultured in hypoxia and anoxia condition. Based on these results, we speculated that there was an interaction between HIF1 α and SENP1, which was further confirmed by Co-IP. To explore the functions of SENP1 in PC3 cells treated with extreme conditions, glycolysis mechanism was examined, and our results displayed that the glucose uptake and LDH releasing were remarkably up-regulated in PC3 cells under hypoxic and anoxic conditions, which indicates that SENP1 might regulate the tumor cell growth by enhancing tumor cell glycolysis. Furthermore, *in vivo* study also confirmed the influence of SENP1 on promoting the tumor progression.

Numerous evidence has demonstrated that SENP1 mediates a diverse array of cellular events by conjugating to the androgen receptor, HIF1 α , c-jun and cyclin D1, etc [26]. In addition, SENP1 has been shown to play to the key role in improving the target protein stability by a SUMOylation machinery. Hence, it also suggests the interaction between SENP1 and HIF1 α regulates the stability of HIF1 α . Our data verified that HIF1 α could be controlled by SENP1, and the deSUMOylation response was implicated in the regulatory mechanism of SENP1.

We also examined the changes of HIF1 α signaling pathway-related proteins in PC3 cells with different treatments. Our results implied that SENP1 might take part in the pathogeneses of prostate cancer by activating HIF1 α signaling pathway, which was consistent with another research [27]. Among the HIF1 α signaling pathway-related proteins, we have verified that MCT4 directly combined with HIF1 α . Thus, according to the results of our study, we proposed that the deSUMOylation response resulted from the interaction of SENP1 and HIF1 α facilitated the stability of HIF1 α which further activated HIF1 α signaling pathway by regulating MCT4 protein and ultimately led to a "Warburg effect".

Taken together, our study firstly verified that SENP1 and HIF1 α interacted with each other to regulate tumorigenesis through up-regulating glycolysis in prostatic carcinoma cells. *In vivo* experiments also showed that SENP1 overexpression could promote tumor cell growth. In addition, the regulatory role of SENP1 on HIF1 α was mainly via a deSUMOylation mechanism and SENP1 might be the key molecule in a "Warburg effect". Hence, SENP1

might be considered as a new therapeutic target for cancer therapy.

Acknowledgments

This work was financially supported by the National Natural Science Foundation of China (Grant No. 81402123).

Ethical approval

All animal experiments were performed according to the Research Ethics Committee of the First Affiliated Hospital of Harbin Medical University guidelines and regulations.

Competing Interests

The authors have declared that no competing interest exists.

References

- Warburg O. On the origin of cancer cells. *Science*. 1956; 123: 309-14.
- Hanahan D, Weinberg RA. Hallmarks of cancer: the next generation. *Cell*. 2011; 144: 646-74.
- Vander Heiden MG, Cantley LC, Thompson CB. Understanding the Warburg effect: the metabolic requirements of cell proliferation. *Science*. 2009; 324: 1029-33.
- Liu W, Kang L, Han J, Wang Y, Shen C, Yan Z, et al. miR-342-3p suppresses hepatocellular carcinoma proliferation through inhibition of IGF-1R-mediated Warburg effect. *Onco Targets Ther*. 2018; 11: 1643-53.
- Osthus RC, Shim H, Kim S, Li Q, Reddy R, Mukherjee M, et al. Deregulation of glucose transporter 1 and glycolytic gene expression by c-Myc. *J Biol Chem*. 2000; 275: 21797-800.
- Kim JW, Gao P, Liu YC, Semenza GL, Dang CV. Hypoxia-inducible factor 1 and dysregulated c-Myc cooperatively induce vascular endothelial growth factor and metabolic switches hexokinase 2 and pyruvate dehydrogenase kinase 1. *Mol Cell Biol*. 2007; 27: 7381-93.
- Teicher BA, Linehan WM, Helman LJ. Targeting cancer metabolism. *Clin Cancer Res*. 2012; 18: 5537-45.
- Erler JT, Cawthorne CJ, Williams KJ, Koritzinsky M, Wouters BG, Wilson C, et al. Hypoxia-mediated down-regulation of Bid and Bax in tumors occurs via hypoxia-inducible factor 1-dependent and -independent mechanisms and contributes to drug resistance. *Mol Cell Biol*. 2004; 24: 2875-89.
- Nenu I, Gafencu GA, Popescu T, Kacso G. Lactate - A new frontier in the immunology and therapy of prostate cancer. *J Cancer Res Ther*. 2017; 13: 406-11.
- Cheng J, Bawa T, Lee P, Gong L, Yeh ET. Role of desumoylation in the development of prostate cancer. *Neoplasia*. 2006; 8: 667-76.
- Bawa-Khalife T, Cheng J, Lin SH, Iltmann MM, Yeh ET. SENP1 induces prostatic intraepithelial neoplasia through multiple mechanisms. *J Biol Chem*. 2010; 285: 25859-66.
- Chandel NS, Simon MC. Hypoxia-inducible factor: roles in development, physiology, and disease. *Cell Death Differ*. 2008; 15: 619-20.
- Li T, Huang S, Dong M, Gui Y, Wu D. Prognostic impact of SUMO-specific protease 1 (SENP1) in prostate cancer patients undergoing radical prostatectomy. *Urol Oncol*. 2013; 31: 1539-45.
- Keating E, Martel F. Antimetabolic Effects of Polyphenols in Breast Cancer Cells: Focus on Glucose Uptake and Metabolism. *Front Nutr*. 2018; 5: 25.
- Tarrado-Castellarnau M, de Atauri P, Cascante M. Oncogenic regulation of tumor metabolic reprogramming. *Oncotarget*. 2016; 7: 62726-53.
- Dong B, Gao Y, Kang X, Gao H, Zhang J, Guo H, et al. SENP1 promotes proliferation of clear cell renal cell carcinoma through activation of glycolysis. *Oncotarget*. 2016; 7: 80435-49.
- Qiu C, Wang Y, Zhao H, Qin L, Shi Y, Zhu X, et al. The critical role of SENP1-mediated GATA2 deSUMOylation in promoting endothelial activation in graft arteriosclerosis. *Nat Commun*. 2017; 8: 15426.
- Siegel RL, Miller KD, Jemal A. Cancer statistics, 2016. *CA Cancer J Clin*. 2016; 66: 7-30.
- Paolicchi E, Gemignani F, Krstic-Demonacos M, Dedhar S, Mutti L, Landi S. Targeting hypoxic response for cancer therapy. *Oncotarget*. 2016; 7: 13464-78.
- Rofstad EK. Microenvironment-induced cancer metastasis. *Int J Radiat Biol*. 2000; 76: 589-605.
- Brown JM, Wilson WR. Exploiting tumour hypoxia in cancer treatment. *Nat Rev Cancer*. 2004; 4: 437-47.
- Chen Z, Lu W, Garcia-Prieto C, Huang P. The Warburg effect and its cancer therapeutic implications. *J Bioenerg Biomembr*. 2007; 39: 267-74.
- Park MH, Bae SS, Choi KY, Min do S. Phospholipase D2 promotes degradation of hypoxia-inducible factor-1 α independent of lipase activity. *Exp Mol Med*. 2015; 47: e196.
- Xia W, Tian H, Cai X, Kong H, Fu W, Xing W, et al. Inhibition of SUMO-specific protease 1 induces apoptosis of astrogloma cells by regulating NF-kappaB/Akt pathways. *Gene*. 2016; 595: 175-9.
- Bettermann K, Benesch M, Weis S, Haybaeck J. SUMOylation in carcinogenesis. *Cancer Lett*. 2012; 316: 113-25.
- Bawa-Khalife T, Yang FM, Ritho J, Lin HK, Cheng J, Yeh ET. SENP1 regulates PTEN stability to dictate prostate cancer development. *Oncotarget*. 2017; 8: 17651-64.
- Wang Q, Xia N, Li T, Xu Y, Zou Y, Zuo Y, et al. SUMO-specific protease 1 promotes prostate cancer progression and metastasis. *Oncogene*. 2013; 32: 2493-8.